Photonic Parton distributions at small x and Regge Cut

Michiko IMOTO and Takashi KIKUCHI

Laboratory of Physics, College of Science and Technology
Nihon University,Funabashi,Chiba 274, Japan

The parton distributions of the photon are obtained in the next-to-leading order (NLO) by imposing a vector-meson dominance(*VMD*) model with the Regge pole behavior or the Regge cut one. Then $F_2^{\gamma}(x,Q^2)$ have a different behavior at small x between the Regge pole input and Regge cut one. The future data will choose either case and decide the structure of the gluon and sea quark distributions at small x and Q_0^2. We find that the contribution of the gluon distribution in the photon structure function is negligible even at small x .

§ 1 Introduction

The photon structure function as measured in the process $e^+e^- \to e^+e^-$ hadrons has the hadronic parts and the point like parts as a result of the dual nature of the photon . The parton distributions constitute the photon structure function and have been obtained by solving the inhomogeneous leading order (LO) or next-to-leading order (NLO) Altarelli-Parisi(A-P) evolution equations.[1),2),3)] At values of Q^2 where the data are taken , the parton distributions depend on the initial condition for the evolution and the starting value of Q^2, Q_0^2. In many cases, Q_0^2 can be taken low enough for $F_2^{\gamma}(x, Q_0^2)$ to be hadronic and the Vector Meson Dominance model(*VMD*) is adopted as the input. Recently it has been analyzed that the hadronic (*VMD*) input dominates the parton distributions in the photon at small x [4)]. This means that depending on the way to choose the input, extrapolations into small x are possible in the framework of the AP equations. However it should be noted that at two loop level the initial condition depends on the factorization schemes. On the other hand, some gluon distributions ,which have systematically different gluon contents[5)] or which have two variants of boundary condition[6)] ,were shown and it was proposed that the photon structure function was sensitive to the gluon distribution only at very small x. Then many authors have used such a way that the parton distributions obtained from the solutions of the inhomogeneous 2-loop AP evolution equations are parametrized , the results of the parametrization are fitted to the experimental data and the gluon distribution for the very small x region has been predicted using this parametrization[7)]. Recently it is shown that the gluon distribution in the photon in LO from the H1

collaboration[8] dose not have a steep rise at small x and the GRV(OL)[7] prediction agrees well with this result. However, at smaller x region($x < 10^{-2}$) one does not know whether it becomes steeply rising or not. The future data will decide it.

In this paper we propose such a representation that the gluon and sea quark distributions show the sensitivity at small x region. First we solve the inhomogeneous A-P equations at the two loop level and discuss about the contribution of the $O(\alpha_s(Q^2))$ term. Next the Regge cut is introduced for the *VMD* input. We show the different behavior for the distributions at small x between sorts of Regge singularities.

§ 2. *Solution of inhomogeneous A-P equation*

In this section we explain the way to calculate the photonic structure function and the parton distributions in the framework of perturbative QCD .

The relation between the observable, $F_2^{\gamma}(x, Q^2)$ and the parton distributions, $q_{NS}^{\gamma}(x,Q^2)$, $\Sigma^{\gamma}(x,Q^2)$ and $G^{\gamma}(x,Q^2)$, is in 2 loop order

$$\frac{1}{x}F_2^{\gamma}(x,Q^2) = q_{NS}^{\gamma}(x,Q^2) + \langle e^2\rangle\Sigma^{\gamma}(x,Q^2)$$
$$+\frac{\alpha_s(Q^2)}{4\pi}B_q(x)*[q_{NS}^{\gamma}(x,Q^2) + \langle e^2\rangle\Sigma^{\gamma}(x,Q^2)]$$
$$+\langle e^2\rangle\frac{\alpha_s(Q^2)}{4\pi}B_G(x)*G_{\gamma}(x,Q^2)+3f\langle e^4\rangle\frac{\alpha}{4\pi}B_{\gamma}(x) \qquad (1)$$

where $\langle e^k\rangle \equiv \frac{1}{f}\sum_q^f e_q^k$, $q_{NS}^{\gamma}(x,Q^2) \equiv \Sigma_f(e_q^2 - \langle e^2\rangle)(q^{\gamma} + \overline{q^{\gamma}})$ for the flavor nonsinglet case and $\Sigma^{\gamma}(x,Q^2) \equiv \Sigma_f(q^{\gamma} + \overline{q^{\gamma}})$ for the flavor singlet case.

The parton distributions for the massless satisfy the following inhomogeneous A-P evolution equations . For the nonsinglet quark distribution

$$\frac{dq_{NS}(n,t)}{dt} = \{1 - \frac{\beta_1}{2\beta_0}(\frac{\alpha_s(t)}{2\pi})\}[(\frac{\alpha_s(t)}{2\pi})^{-1}P_{q\gamma}^0(n) + P_{q\gamma}^1(n)\}] +$$
$$+[P_{qq}^{(0)}(n) + (\frac{\alpha_s(t)}{2\pi})R_{NS}(n)]q(n,t) \qquad (2)$$

where the moment representation is defined by $f(n,t) = \int_0^1 x^{n-1}f(x,t)dx$ and is adopted for the parton distributions $q_i(x,t)$ and the splitting functions $P_{ij}(x,t)$[9] and $P_{i\gamma}(x,t)$[10] in the x space .

Similarly for the singlet and the gluon distributions

$$\frac{d\Sigma(n,t)}{dt} = \frac{\alpha'}{2\pi}\{(\frac{\alpha_S(t)}{2\pi})^{-1} P_{qr}{}^{(0)}(n) + P_{qr}(n)^{(1)}(n)\}\{1 - \frac{\beta_1}{2\beta_0}(\frac{\alpha_S(t)}{2\pi})\} + \{P_{qq}^{(0)}(n) + \frac{\alpha_S(t)}{2\pi} R_{qq}(n)\}\Sigma(n,t)$$

$$+\{P_{qG}^{(0)}(n) + \frac{\alpha_S(t)}{2\pi} R_{qG}(n)\}G(n,t), \tag{3}$$

$$\frac{dG(n,t)}{dt} = \frac{\alpha'}{2\pi}\{1 - \frac{\beta_1}{2\beta_0}(\frac{\alpha_S(t)}{2\pi})\}P_{G\gamma}(n)^{(1)} + \{P_{Gq}^{(0)}(n) + \frac{\alpha_S(t)}{2\pi} R_{Gq}(n)\}\Sigma(n,t)$$

$$+.\{P_{GG}^{(0)}(n) + \frac{\alpha_S(t)}{2\pi} R_{GG}(n)\}G(n,t) \tag{4}$$

where $R_{ij}(n) = P_{ij}^{(0)}(n) - (\beta 1 / 2\beta 0) P_{ij}^{(1)}(n)$ for ij=(NS,qq,qG,Gq,GG). Here the $O(\alpha_S(t)^2)$ terms are truncated in the expansion of the splitting functions $P_{ij}(x,t)$ and $P_{i\gamma}(x,t)$ as power series in $\alpha_S(t)$..Then α'=1/137, t=(1/2)ln($\alpha_S(Q_0^2)$ / $\alpha_S(Q^2)$) and $\alpha_S(Q^2)$ satisfies $d\alpha_S(Q^2)/d\ln Q^2 = -\beta_0(\alpha_S(Q^2)/4\pi) - \beta_1(\alpha_S(Q^2)/4\pi)^2$ with β_0=11-2 f /3 and β_1=102- 38 f /3, where f is the number of flavors.

In our case, the $O(\alpha_S(Q^2))$ terms are remained in the inhomogeneous terms, too. **The solution of the above equation is obtained as a superposition of a general solution of the homogeneous equations (without the photonic parton splitting function terms) and a particular solution of the inhomogeneous equation. The former is a hadron-like part distribution , $q_H(n,x)$ where the photon turns into a bound $q\bar{q}$ state through an effective coupling to a vector meson like state. And the latter is a point-like part one, $q_{PL}(n,x)$ where the photon has a point like coupling to a $q\bar{q}$ pair.**

The solution for the nonsinglet equation is expressed to be

$$q_{NS}(n,Q^2) = q_{NS,H}(n,Q^2) + q_{Ns,P.L}(n,Q^2)\ , \tag{5}$$

where

$$q_{NS,PL}(n,Q^2) = \frac{\alpha'}{2\pi}[\{a_{11}(n)\frac{1-L^{1-\frac{2}{\beta_0}P_{qq}^{(0)}(n)}}{1-\frac{2}{\beta_0}P_{qq}^{(0)}(n)}\}(\frac{\alpha_S(Q^2)}{2\pi})^{-1}$$

$$+\{a_{12}(n)\frac{1-L^{1-\frac{2}{\beta_0}P_{qq}^{(0)}(n)}}{1-\frac{2}{\beta_0}P_{qq}^{(0)}(n)} + a_{21}(n)\frac{1-L^{-\frac{2}{\beta_0}P_{qq}^{(0)}(n)}}{-\frac{2}{\beta_0}P_{qq}^{(0)}(n)}\}(\frac{\alpha_S(Q^2)}{2\pi})^{0}$$

$$+a_{22}(n)\frac{1-L^{-\frac{2}{\beta_0}P_{qq}^{(0)}(n)}}{-\frac{2}{\beta_0}P_{qq}^{(0)}(n)} + a_{31}(n)\frac{1-L^{-1-\frac{2}{\beta_0}P_{qq}^{(0)}(n)}}{-1-\frac{2}{\beta_0}P_{qq}^{(0)}(n)}\}(\frac{\alpha_S(Q^2)}{2\pi})^{1}] \tag{6}$$

where $L = \frac{\alpha_S(Q^2)}{\alpha_S(Q_0^2)}$.

And the solutions for the singlet quark and qluon simultaneous equations are

$$\Sigma_{PL}(n,Q^2)=(\frac{\alpha'}{2\pi})\,[\,\{\,b_{11}(n)\frac{1-L^{1-\frac{2}{\beta_0}\lambda_1(n)}}{1-\frac{2}{\beta_0}\lambda_1(n)}\,\}\,(\frac{\alpha_S(Q^2)}{2\pi})^{-1}$$

$$+\{\,b_{12}(n)\frac{1-L^{1-\frac{2}{\beta_0}\lambda_1(n)}}{1-\frac{2}{\beta_0}\lambda_1(n)}+b_{21}(n)\frac{1-L^{-\frac{2}{\beta_0}\lambda_1(n)}}{-\frac{2}{\beta_0}\lambda_1(n)}\,\}\,(\frac{\alpha_S(Q^2)}{2\pi})^{0}$$

$$+\{\,b_{22}(n)\frac{1-L^{-\frac{2}{\beta_0}\lambda_1(n)}}{-\frac{2}{\beta_0}\lambda_1(n)}+b_{31}(n)\frac{1-L^{-1-\frac{2}{\beta_0}\lambda_1(n)}}{-1-\frac{2}{\beta_0}\lambda_1(n)}\,\}\,(\frac{\alpha_S(Q^2)}{2\pi})^{1}\,]$$

$$+(\frac{\alpha'}{2\pi})\,[\,\lambda_1\leftrightarrow\lambda_2\,] \qquad (7)$$

$$G_{PL}(n,Q^2)=(\frac{\alpha'}{2\pi})\,[\,\{\,c_{11}(n)\frac{1-L^{1-\frac{2}{\beta_0}\lambda_1(n)}}{1-\frac{2}{\beta_0}\lambda_1(n)}\,\}\,(\frac{\alpha_S(Q^2)}{2\pi})^{-1}$$

$$+\{\,c_{12}(n)\frac{1-L^{1-\frac{2}{\beta_0}\lambda_1(n)}}{1-\frac{2}{\beta_0}\lambda_1(n)}+c_{21}(n)\frac{1-L^{-\frac{2}{\beta_0}\lambda_1(n)}}{-\frac{2}{\beta_0}\lambda_1(n)}\,\}\,(\frac{\alpha_S(Q^2)}{2\pi})^{0}$$

$$+\{\,c_{22}(n)\frac{1-L^{-\frac{2}{\beta_0}\lambda_1(n)}}{-\frac{2}{\beta_0}\lambda_1(n)}+c_{31}(n)\frac{1-L^{-1-\frac{2}{\beta_0}\lambda_1(n)}}{-1-\frac{2}{\beta_0}\lambda_1(n)}\,\}\,(\frac{\alpha_S(Q^2)}{2\pi})^{1}\,]+(\frac{\alpha'}{2\pi})\,[\,\lambda_1\leftrightarrow\lambda_2\,], \qquad (8)$$

where $a_{ij}(n), b_{ij}(n)$ and $c_{ij}(n)$ are recorded in Appendix and

$$\lambda_{1,2}(n)=\frac{1}{2}[(P_{qq}^{(0)}(n)+P_{GG}^{(0)}(n))\pm\{(P_{qq}^{(0)}(n)-P_{GG}^{(0)}(n))^2+4P_{qG}^{(0)}(n)P_{Gq}^{(0)}(n)\}^{\frac{1}{2}}]. \qquad (9)$$

For the above solutions, first we have confirmed numerically that the above parton distributions except the $O(\alpha_S(Q^2))$ terms produce the same result as the point like parts of distributions shown in ref.(1) and that the n- moment of the distributions at $Q^2\to\infty$ are independent of the values Q_0^2 . Also the solutions in leading order are entailed in the above expressions by taking $R_{NS}(n)$, $R_{ij}(n)\to 0$, $\beta_1(n)\to 0$ and $P_{NS}^{(1)}$, $P_{ij}^{(1)}(n)\to 0$ in eq.(6),(7) and eq.(8).

Next the point-like parts of the above solutions have explicitly simple poles for each order term at the following values n^m of n which we calculated for f=3. They are n^m

=0.385(NS) and n^m = 1.725(S,G) for the $O(\alpha_s(Q^2)^{\cdot 1})$ term, n^m =1.0(NS) and n^m =2.0(S,G) for $O(\alpha_s(Q^2)^0)$ and n^m=6.0(NS), $n^m(\lambda_1)$=7.0(S,G) and $n^m(\lambda_2)$=3.0(S,G) for $O(\alpha_s(Q^2))$. As mentioned in ref.(11), when the solutions in n-space are transformed into x-space by the inverse Mellin transform ,these n-poles correspond to the origin singularities of the form$(1/x)^{n^m}$ at x-space. So the introduction of the $O(\alpha_s(Q^2))$terms makes the behavior of the power singularities severer. It should, however, be noted that in eq.(6),(7) and eq.(8) these singularities are canceled by vanishing numerators at the same points and are replaced by the logarithmic divergence at $\alpha_s(Q^2)\to 0$, since $\lim_{A\to 0}\frac{1}{A}[1-L^A]=-\ln L$.

Then we examine numerically the contribution of the each order term in $\alpha_s(Q^2)$ for the point-like parton distributions , $q_{NS,PL}(n,Q^2)$, $\Sigma_{PL}(n,Q^2)$ and $G_{PL}(n,Q^2)$. Here we work with the $\overline{MS}$ scheme and adopt Q^2 = 15 GeV^2,Q_0^2 =1 GeV^2, Λ=200MeV and f=3. We find that the contribution of the $O(\alpha_s(Q^2))$ term is about 12% of the NLO approximation for the G(n=4,Q^2) in contrast with its negligible contribution for the point-like quark distributions, $q_{NS,PL}(n,Q^2)$ and $\Sigma_{PL}(n,Q^2)$. Here the contribution of the $O(\alpha_s(Q^2))$ term should be considered beyond the NLO approximation, but we suggest the importance of this contribution for the gluon distribution at small x.

§ 3 *The Regge cut in the input distribution.*

The recent study of the proton structure function at small x have offered the important pieces of information theoretically or experimentally. One of them is that the gluon and sea quark distributions increase with decreasing x and the input parton distributions dominate them at small x[12),13)]. Here, in line with this results we modify the photonic input distributions at the value Q_0^2, q(n,Q_0^2), Σ(n,Q_0^2) and G(n,Q_0^2) and prepare the representation to predict the future data of the photonic structure function at small x .

Then we estimate the hadronic input distributions using *VMD* arguments, as is commonly done, and adopt Q_0^2 = 1 GeV^2 at which the *VMD* model is in good agreement with the measured total γ - γ cross section. . The *VMD* photon structure function is defined as

$$F_{2,VMD}^{\gamma} = \frac{4\pi\alpha'}{f_\rho^2}\Sigma\, e_i^2 x q_i^{\rho}(x,Q_0^2), \tag{10}$$

where $f_\rho^2/4\pi$=2.2 and we assume that the quark distributions in the ρ^0 meson, q_i^{ρ} (x,Q_0^2), can be represented by the sum of corresponding distributions in $\pi^{\pm}$ mesons. The pion distributions are expressed in terms of valence quark, v^{π}, and sea

quark ζ^{π} distributions, so we obtain

$$F_{2,VM}{}^{\gamma} = \frac{4\pi\alpha'}{f_\rho^2}\left(\frac{5}{9}v^{\pi} + \frac{4}{3}\zeta^{\pi}\right). \tag{11}$$

Then above input distributions follows,

$$q^{\gamma}(x,Q_0^2) = \frac{4\pi\alpha'}{f_\rho^2}\left(\frac{1}{9}v^{\pi}\right)$$

$$\Sigma^{\gamma}(x,Q_0^2) = \frac{4\pi\alpha'}{f_\rho^2}(2v^{\pi} + 6\zeta^{\pi}), \tag{12}$$

while $G^{\gamma}(x,Q_0^2)$ affect the evolution to higher Q^2 at very small x and are expressed as

$$G^{\gamma} = \frac{4\pi\alpha'}{f_\rho^2}G^{\pi}(Q_0^2,x),$$

For the pion parton distributions, many authors have used the form given in ref.(3),

$$x v^{\pi}(x) = A\sqrt{x}(1-x), \quad x\zeta^{\pi}(x) = B(1-x)^5 \quad \text{and} \quad xG^{\pi}(x) = C(1-x)^3, \tag{13}$$

where the each power of x is chosen in line with Regge pole exchange theory and the power of (1-x) is in line with counting rules[14]. Regge pole exchange is a generalization of a single particle exchange. The Regge poles are characterized by quantum numbers like charge ,isospin, strangeness, G parity, etc. The Regge poles carrying the quantum numbers of the vacuum are called the Pomeron (P) with $\alpha_P(0)=1$ and Igi-pole (P').with $\alpha_P(0)=1/2$. Also Regge-pole exchange is represented in terms of quarks and gluons. The exchange of $q\bar{q}$ bound states corresponding to the exchange of mesons can be related to the Regge pole, while the Pomeron can be thought of as corresponding to an exchange of a pair of gluons. In addition to the exchange of a single Reggeon or Pomeron, it is also possible to exchange more Reggeons or Pomerons simultaneously. This gives rise to Regge cuts. The high-energy behavior of a two-body amplitude due to Regge-pole exchange or Regge cut is

$$A^R(s,t) \underset{s\to\infty}{\approx} s^{\alpha_R(t)} \quad \text{or} \quad A^C(s,t) \underset{s\to\infty}{\approx} \frac{s^{\alpha_c(t)}}{\log s} \quad .$$

Here, using $s=Q^2(1-x)/x$, (the relation of the canonical Bjorken variable, x and the second power of the energy of the hadronic system produced in γ - γ reaction, s), we can adopt the asymptotic form $x^{1-\alpha_R(0)}$ or $x^{1-\alpha_C(0)}/\ln(1/x)$ for the gluon and sea quark distributions in eq. (13) . Then we obtain the following forms for the gluon distributions by the sort of Regge singularities,

$$xG^{\pi}(x) = C x^{1-\alpha_R(0)}(1-x)^3 \quad : \text{(Regge Pole)}, \tag{14a}$$

$$xG^{\pi}(x) = C(x^{1-\alpha_R(0)} + x^{1-\alpha_C(0)} / \ln(1/x))(1-x)^3 \quad : \text{(Regge Pole + Regge Cut)}, \tag{14b}$$

$$xG^{\pi}(x) = C(x^{1-\alpha_C(0)} / \ln(1/x))(1-x)^3 \quad : \text{(Regge Cut)}. \tag{14c}$$

where $\alpha_c(t) = max.\{\alpha_{R_1}(t) + \alpha_{R_2}(t) - 1\}$ gives the position of the branch point trajectory and we take the same form into the Regge part of $x\zeta^{\pi}(x)$ in eq.(13),too.

Here, as the powers of Regge pole become zero with unit Pomeron intercept for $x\zeta^{\pi}(x)$ and $xG^{\pi}(x)$,one can not express rigorously their aspect in the very small x ($x \approx 0$) region, Therefore we introduce the Regge cut contribution to such distributions and present the different hadronic structure in the photon by the sort of Regge singularities, P pole, P pole + P-P' cut and P-P' cut, for $xG^{\pi}(x)$ and $x\zeta^{\pi}(x)$.

Fig.1 shows the photon structure function calculated by using our modified VMD model for $Q^2=15GeV^2$, as a function of x. Although we find that the differences between the predictions by the sorts of Regge singularities are negligibly small at the region where the data are taken, from fig.2 we find the differences between them at small x. Our ,P pole, P pole + P-P' cut and P-P' cut predictions for $xG^{\gamma}(x)$ are compared in fig.3 which shows that the rising of $xG^{\gamma}(x)$ with P-P' cut is steeper than the other one at small x. In contrast with this prediction, the structure function with P-P' cut in fig.2 runs under one with the other Regge singularities. This situation is caused by that the contribution of $\Sigma(x,Q^2)$ dominates even at very small x and has sensitivity to the different sorts of Regge singularity introduced in the nonperturbative sea quark distribution.

In the end we make an additional remark that adopting $\alpha_P(0) \cong 1.08$, we get Lipatov behavior , $x^{-\lambda}$ from P-P cut

Here A is determined as A =0.75 from the net number of quarks in the meson and B , C are chosen as B=0.1, C=2 from the momentum conservation[3] with the gluons taking 50% of momentum which the valence quarks carry .

Also the x-space distributions, $f((x,Q^2)$ can be obtained by performing the inverse Mellin transformation from the moment-n space one, $f((n,Q^2)$:i.e.,

$$f(x,Q^2) = \frac{1}{\pi}\int_0^{\infty} dz\, \mathrm{Im}[e^{i\varphi}x^{-c-ze^{i\varphi}} f(n = c + ze^{i\varphi}, Q^2)] \tag{15}$$

where the following contour of integration is chosen[1]

$$\varphi = \frac{3}{4}\pi,$$

c=0.8 for nonsinglet,

c=1.8 for singlet, gluon.

§ 4 *Discussion*

In this paper, we have proposed the representations of $G(x,Q^2)$ and $\zeta(x,Q^2)$ being sensitive to x at small x. We have found that the photon structure function does not have the sensitivity to $G(x,Q^2)$ even at very small x. However our predictions for $F_2^{\gamma}(x,Q^2=15)$ show lower values than the experimental data. For this problems we will try to improve as follows,

1) the charm contribution to the photon structure function : It should be taken into account only if $W^2 > 4m_c^2$, where m_c is the mass of the charm quark and W is the invariant mass of the photon-photon system. In $Q^2 = 15$, the region satisfying this constraint is at all $x < 0.625$.
2) the gluons carrying the less momentum than 50% of momentum which the valence quarks carry : As $G(x,Q^2)$ and $\zeta(x,Q^2)$ are correlative, it is possible to increase the contribution of $\Sigma(x,Q^2)$ for $F_2^{\gamma}(x,Q^2)$ by increasing momentum for $\zeta(x,Q^2)$ to carry.

Next, we have calculated the parton distributions at small x using the A-P evolution equation, since the hadronic (VDM) input dominates the parton distributions at small x. In fact, the A-P evolution equation instead of the BFKL equation have been used for the proton structure function in the HERA region[12]with conditions attached. We will study about this condition for our case.

Appendix

The coefficients $a_{ij}(n)$ for $q_{PL}(n,Q^2)$ are as follows,

$$a_{11}(n)=\frac{2}{\beta_0}P_{NS\gamma}^{(0)}(n)$$

$$a_{12}(n)=-(\frac{2}{\beta_0})R_{NS}(n)$$

$$a_{21}(n)=-(\frac{2}{\beta_0})(T(n)P_{NS\gamma}^{(0)}(n)-P_{NS\gamma}^{(1)}(n))$$

$$a_{22}(n)=(\frac{2}{\beta_0})^2 R_{NS}(n)(T(n)P_{NS\gamma}^{(0)}(n)-P_{NS\gamma}^{(1)}(n))$$

$$a_{31}(n)=-(\frac{2}{\beta_0})R_{NS}(n)P_{NS\gamma}^{(0)}+T(n)P_{NS\gamma}^{(1)}(n))$$

where T(n)=$\frac{\beta_1}{2\beta_0}-\frac{2}{\beta_0}R_{NS}(n)$. For the singlet quark and the gluon distributions, we have to solve the simultaneous inhomogeneous evolution equations, eqs.(2) and (3). Then we eliminate $G_H(n,t)$ from the homogeneous equations for eqs(2) and (3) and get the following equation,

$$\frac{d^2\Sigma_{\rm H}(n,t)}{dt^2}-p(n,t)\frac{d\Sigma_{\rm H(}(n,t)}{dt}+q(n,t)\Sigma_{\rm H}(n,t)=0 \qquad \text{(A-1)}$$

where

$$p(n,t)=p_0(n)+p_1(n)\frac{\alpha(t)}{2\pi}$$

with

$$p_0(n)=P_{qq}^{(0)}(n)+P_{GG}^{(0)}(n),$$

$$p_1(n)=\frac{2}{\beta_0}(R_{qq}(n)+R_{GG}(n))\ -(P_{qG}^{(0)}(n))^{-1}R_{qG}(n)$$

and

$$q(n,t)=q_0(n)+q_1(n)\frac{\alpha(t)}{2\pi}$$

with

$$q_0(n)=P_{qq}^{(0)}(n)P_{GG}^{(0)}(n)-P_{qG}^{(0)}(n)P_{Gq}^{(0)}(n)$$

$$q_{1}(n)=R_{qq}(n)-(P_{qG}^{(0)}(n))^{-1}R_{qG}(n)\ +\frac{2}{\beta_0}(P_{GG}^{(0)}(n)R_{qq}(n)+P_{qq}^{(0)}(n)R_{GG}(n)$$
$$-P_{qG}^{(0)}(n)R_{Gq}(n)-P_{Gq}^{(0)}(n)R_{qG}(n)).$$

As the solution of eq.(A-1) we have

$$\Sigma_H(n,t) = A(\lambda_1,t)e^{\lambda_1(n)t} + A(\lambda_2,t)e^{\lambda_2 n)t}$$

where

$$A(\lambda,\tau) = K_1(\lambda) + K_2(\lambda)\frac{\alpha(t)}{2\pi}$$

with

$$K_1(\lambda) = \frac{\beta_0}{2} - 2\lambda(n) + p_0(n)$$

$$K_2(\lambda) = \lambda(n)p_1(n) - q_1(n).$$

Substituting the above solution for the Gluon homogeneous equation, we obtain the homogeneous solution,

$$G_H(n,t) = B(\lambda_1,t)e^{\lambda_1(n)t} + B(\lambda_2,t)e^{\lambda_2 n)t}$$

where

$$B(\lambda,\tau) = L_1(\lambda) + L_2(\lambda)\frac{\alpha(t)}{2\pi}$$

with

$$L_1(\lambda) = (P_{qG}^{(0)}(n))^{-1}K_1(\lambda)(\lambda(n) - P_{qq}^{(0)}(n))$$

$$L_2(\lambda) = -(P_{qG}^{(0)}(n))^{-1}[(\frac{\beta_0}{2} - \lambda(n) + P_{qq}^{(0)}(n))K_2(\lambda)$$

$$+(P_{qG}^{(0)}(n)R_{qq}(n) + \lambda(n)R_{qG}(n) - P_{qq}^{(0)}(n)R_{qG}(n))\frac{K_1(\lambda)}{P_{qG}^{(0)}(n)}.$$

Then we define $b_{ij}(n)$ in eq.(6) and $c_{ij}(n)$ in eq(7) as follows

$$b_{ij}(n) = H_i(\lambda_2(n))K_j(\lambda_1(n))$$

$$c_{ij}(n) = H_i(\lambda_2(n))L_j(\lambda_1(n))$$

where

$$H_1(\lambda) = P_{q\gamma}^{(0)}(n)\ \ L_1(\lambda)$$

$$H_2(\lambda) = P_{q\gamma}^{(0)}(n)[L_2(\lambda) - S(\lambda_1,\lambda_2)L_1(\lambda) + P_{q\gamma}^{(1)}(n)L_1(\lambda) - P_{G\gamma}^{(1)}(n)K_1(n)$$

$$H_3(\lambda) = -P_{q\gamma}^{(0)}(n)[S(\lambda_1,\lambda_2)L_2(\lambda) + (\frac{Z(\lambda_1,\lambda_2)}{X(\lambda_1,\lambda_2)} - \frac{Y(\lambda_1,\lambda_2)}{X(\lambda_1,\lambda_2)}S(\lambda_1,\lambda_2))L_1(\lambda)]$$

$$+P_{q\gamma}^{(1)}(n)[L_2(\lambda) - S(\lambda_1,\lambda_2)L_1(\lambda)]\ \ -P_{G\gamma}^{(1)}(n)[K_2(\lambda) - S(\lambda_1,\lambda_2)K_1(\lambda)]$$

with

$$X(\lambda_1,\lambda_2) = K_1(\lambda_1)L_1(\lambda_2) - (\lambda_1 \leftrightarrow \lambda_2)$$

$$Y(\lambda_1,\lambda_2) = K_1(\lambda_1)L_2(\lambda_2) + L_1(\lambda_2)K_2(\lambda_1) - (\lambda_1 \leftrightarrow \lambda_2)$$

$$Z(\lambda_1,\lambda_2) = K_2(\lambda_1)L_2(\lambda_2) - (\lambda_1 \leftrightarrow \lambda_2)$$

$$S(\lambda_1,\lambda_2) = \frac{Y(\lambda_1,\lambda_2)}{X(\lambda_1,\lambda_2)} + \frac{\beta_1}{2\beta_0}.$$

References

1)M.Gluck,E.Reya and A.Vogt,Phys.Rev.D45(1992),3986.

2)M.Gluck,K.Grassie and E.Reya,Phys.Rev.D30(1984),1447.
J.H.Field,F.Kapusta and L.Poggioli,Z.Phys.C36(1987)121.

3)J.H.Da Luz Vieira and J.K.Storrow,Z. Phys. C51,(1991),241.
J.F.Owens and E.Reya,Phys.Rev.D17(1978),3003.

4)P.Aurenche,J.P.Guillet and M.Fontannaz,Z.Phys.C64(1994),621.

5)K.Hagiwara,M.Tanaka,I.watanabe and T.Izubuchi,Phys. Rev. D51(1995), 3197.

6)B.L.Ioffe and A.Oganessian,Z.Phys.C69(1995),119.

7)M.Gluck,E.Reya and A.Vogt,Phys.Rev.D46(1992),1973.
H.Abramowicz,K.Charchula and A.Levy,Phys.Lett.B269(1991),458.

8)H1 Collab.,T.Ahmed et al., Nucl.Phys.B445,(1995)195.

9)G.FloraE.tos, C.Kounnas and R.Lacaze, Nucl. Phys.B192,(1981),417.

10)M. Fontannaz and E.Pilon, Phys.Rev.D45(1992),382.

11)G.Rossi,Phys.Rev.D29(1983),852.

12)R.K.Ellis,Z.Kunszt and E.M.Levin, Nucl.Phys.B420,(1994)517.

13)M.Gluck,E.Reya and A.Vogt,Z.Phys.C67(1995),433.

14)G.R.Farrar,Nucl.Phys.B77,(1974)429.
J.F.Gunion,Phys.Rev.D10,(1974),242.

Figure Caption

Fig.1. The comparison between our predictions of F_2^{γ} for $Q^2=15GeV^2$.
The Ppole contribution is shown by solid lines. The pole + P-P' cut and the P-P' cut are shown by dashed lines and by dotted lines, respectively.

Fig.2. At very small x region, the comparison between our predictions in Fig.1.

Fig.3. The small x behavior of $G^{\gamma}(x)$ for $Q^2=15\ GeV^2$; The Ppole contribution is shown by solid lines. The Ppole + P-P cut and the Ppole + P-P' cut are shown by dashed lines and by dotted lines, respectively.

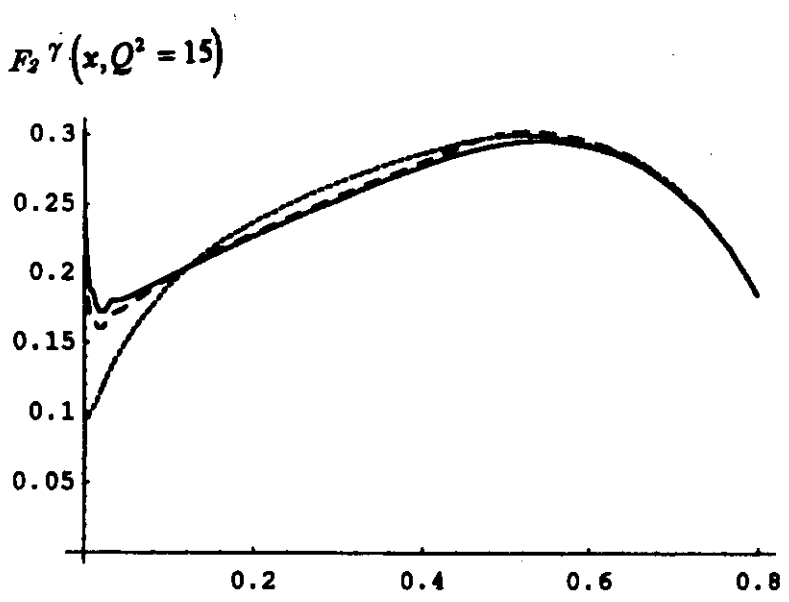

Fig.1. The comparison between our predictions of F_2^{γ} for Q^2=15GeV^2. The Ppole contribution is shown by solid lines. The pole + P-P' cut and the P-P' cut are shown by dashed lines and by dotted lines, respectively.

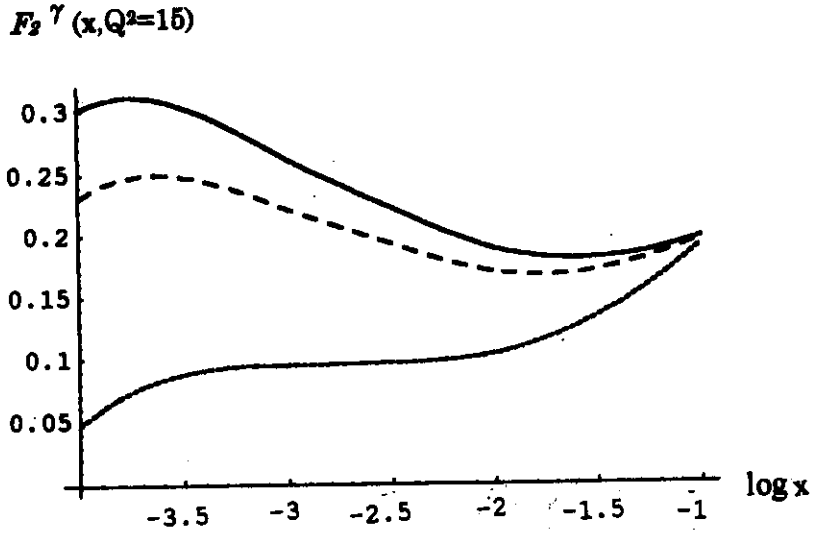

Fig.2. At very small x region, the comparison between our predictions in Fig.1.

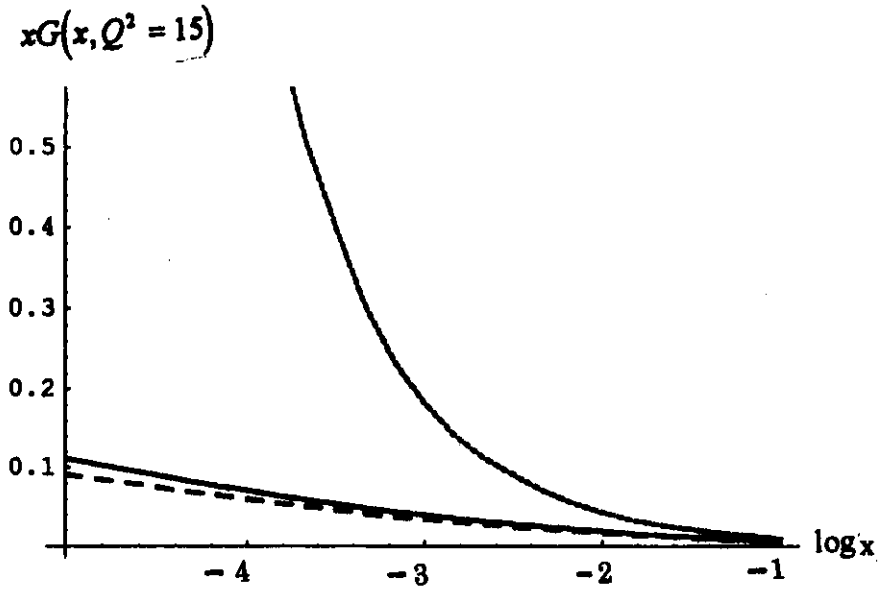

Fig.3. The small x behavior of $G^{\gamma}(x)$ for Q^2=15 GeV^2 ; The Ppole contribution is shown by solid lines. The Ppole + P-P cut and the Ppole + P-P' cut are shown by dashed lines and by dotted lines, respectively.